RETRIEVAL AND VALIDATION OF SEA ICE CONCENTRATION FROM AMSR-E/AMSR2 IN POLAR REGIONS

Qian Shi[1], Jie Su[1]*
Physical Oceanography Laboratory/CIMST, Ocean University of China and Qingdao National Laboratory for Marine Science and Technology, Qingdao, 266100, China

ABSTRACT

Sea ice concentration (SIC) is an important sea ice parameter of the atmosphere-ice-ocean system in the polar region. Daily 6.25 km AMSR-E/AMSR2 SIC from Bremen University (UB) is one of the widely used SIC products. In this paper, MODIS data and aerial image are used to validate this product. The results show that the daily mean AMSR-E ASI products underestimate SICs about 17.9% based on the aerial image, and underestimate SICs about8.5% based on MODIS image. The sea ice extent (SIE) and sea ice area (SIA) which are derived from SIC by ASI algorithm, Dynamic Tie-point ASI algorithm (DT-ASI) as well as NT algorithm are compared.

Index Terms— Sea ice concentration, Retrieval, Validation, AMSR-E, MODIS, aerial image

1. INTRODUCTION

The Arctic sea ice extent (SIE) and sea ice area (SIA) in recent years have a rapid decline in response to global warming [1]. The decreasing rate of SIE and SIA have shifted from about 2.2%/decade and 3.0%/decade in 1979–1996 to about 10.1%/decade and 10.7%/decade during 1997-2007, respectively [2]. The last six years (2007–2012) have been witnessed the six lowest September SIEs on record [3]. According to the remote sensing data from passive microwave, SIEs from different algorithms are basically consistent. However, there are large differences of SIAs since their accuracies are more dependent on the algorithms of SIC. To find the natural phenomena of SIA in polar regions, SIC products need to be validated. SIC is an important parameter for polar sea ice monitoring. Based on 89GHz AMSR-E (Advanced Microwave Scanning Radiometer for Earth Observing System) data, a gridded passive microwave sea ice concentration product can be obtained using the ASI (the Arctic Radiation and Turbulence Interaction Study (ARTIST) Sea Ice) retrieval algorithm [4]. This data, with a relatively higher resolution, became one of the widely used SIC products. Hao and Su (2015) developed the ASI algorithm based on daily changed tie points, which is called as the Dynamic Tie point ASI algorithm (abbreviate as DT-ASI algorithm) [5].

Previous validation work on AMSR-E ASI SIC products show that the bias on first-year ice and young ice region in the Arctic is only between -1% and 4%; However, in the new ice zone along the edge of pack ice, the product presents a seasonal characteristic which overestimated SICs in winter and underestimated SICs in summer [7]. This underestimate could approach -13.62% and 8.90% based on ship-based observations [8] and visible light images, respectively [9]. In this paper, the AMSR-E ASI SIC results are validated by inversed SICs from aerial image and MODIS image in the front of Antarctic Amery Ice Shelf. In addition, the SIE and SIA results of three different algorithms will be the compared in the Arctic, since DT-ASI algorithm has not be applied in the Antarctic.

2. DATA

The objective of SIC validation gridded daily mean AMSR-E SICs from Bremen University with a spatial resolution of 6.25 km. Currently, these data could be download from Bremen University data center: https://seaice.uni-bremen.de/data/.

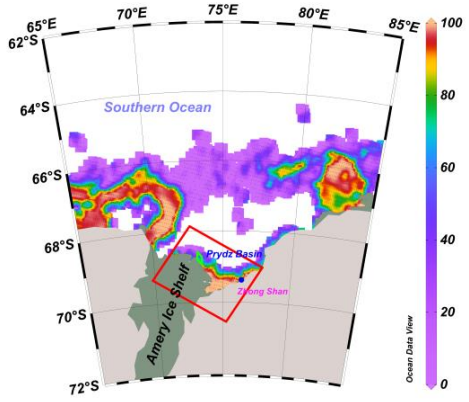

Fig. 1. SIC distribution from Bremen University in front of Amery Ice Shelf on January 9, 2011

During research region, the Prydz Bay was covered by open water, and there is float ice along the edge of Amery Ice Shelf (background color in Fig.1). Red rectangle depicts a range of the sub-MODIS image that is used to

validate ASI SICs. Small green quadrangle depicts the region of aerial photographs. The aerial survey started at 2:40 UTC on January 9th, 2011, lasting 3.5 hours. The camera was anchored under the bottom of the helicopter. The average flight altitude and speed of the helicopter is 800 m and 140km/h. This survey totally acquired about one hundred (100) images with a resolution of 5440 × 4080 pixels. The distance between adjacent images is 240 m and the overlap ratio is approximately 65%. The spatial resolution of the composite image (Fig. 2a) is about 3.82 m, covering an area of 526 km2. The geolocation of the composite image was calibrated based on three fixed points located on the ice shelf. The position error is less than one meter.

Moderate Resolution Imaging Spectroradiometer (MODIS) aboard on the Aqua satellite is synchronized with AMSR-E, making it an optimal tool for validating AMSR-E SIC product [4]. The L1 reflectance data are used for retrieve SIC in this paper.

Daily AMSR2 Level 1B swath brightness temperature data from JAXA (Japan Aerospace Exploration Agency) are used and projected on the polar stereographic grid with the same spatial resolution as ASI products of Bremen University. In Section 3.3 we estimate SIAs and SIEs derived from SICs using DT-ASI algorithm [5].

3. RESULTS

3.1 Validation of AMSR-E ASI SIC using composite aerial Images

In the composite true-color aerial image (Fig. 2a), the ice shelf is located in the southwest, and the floating ice winded roughly northwest-southeast along the edge of the ice shelf. In addition, open water covers north-east part of the image. The optical properties of the ice shelf are close to the thick ice with dry snow and are brighter than typical pack ice in the summertime. If the ice shelf is included in classification criterion, some darker pack ice will be recognized as open water and underestimated SICs of the aerial photo. Therefore, the ice shelf was excluded before discrimination of ice and water. MINERROR threshold algorithm [10], which assumes that gray value (0 ~ 255) histogram of objective image obeys the bimodal Gaussian distribution, was employed in the red, green and blue channel to distinguish sea ice and water in the composited image. The threshold value of the corresponding channel obtained by MINERROR method is 118,141,140, respectively. If grey values of all three channel are greater than the corresponding threshold, the pixel is labeled as ice while the rest pixels are labeled as water.

The discrimination results were given in Fig.2b. Compared with the original panel (Fig.2a), the discriminated result maximizes the keeping characteristics of trash ice and especially recognize those pixels with high reflectance among open waters (in the upper right in Fig. 2a) reasonably, and basically guarantee the reliability of aerial image SICs.

The discriminated aerial binary image is projected onto the AMSR-E (6.25 km) grid, and the ice pixel number in two kinds grids was summarized to calculate the value of SICs of aerial image corresponding in AMSR-E grid. These results are used to validate the AMSR-E ASI SICs.

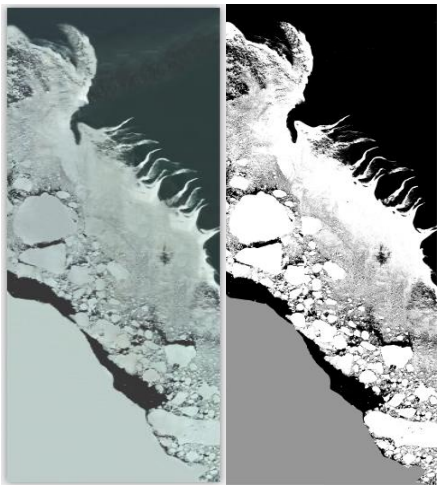

(a) (b)

Fig. 2. (a) Mosaic true-color aerial image on January 9th, 2011; (b) Ice-water binary image after threshold discrimination. Black/white/grey color denotes open water/sea ice/ice shelf, respectively.

Fig. 3 gives a point-by-point comparison between aerial SICs from aerial image and AMSR-E SICs from Bremen University. Only 10 AMSR-E grids are overlapped by the aerial image. Grid No.1-3 represent ice shelf; Grid No.4-6 represent high SIC region mixed by pack ice and trash ice; Grid 7-10 represent relatively low SICs region with trash ice close to open water directly.

SICs of UB SICs is 17.9% lower than that of the aerial image on average. The maximum bias in the ice shelf area was -11%, and the mean bias was 4%; In the high SIC area with large-scale floating ice and trash ice, the average AMSR-E SIC is 47.3%, and the bias (relative error) is -33% (-41%);

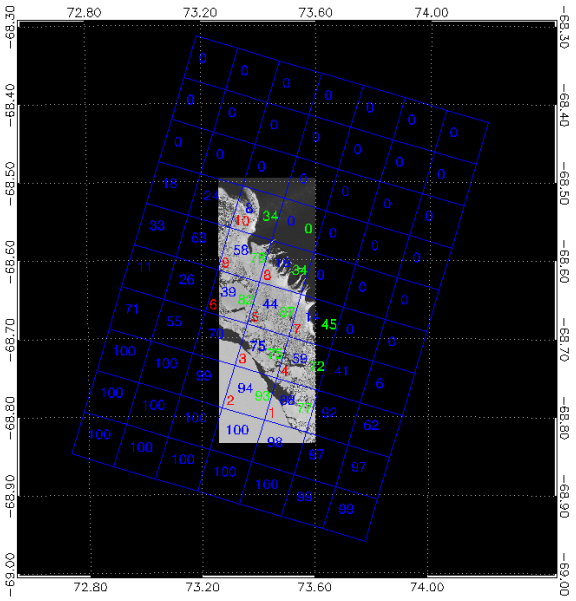

Fig.3. Mosaic SIC distribution on the polar grid based on the Bremen University AMSR-E SIC data. Red number with 0-10 denotes grid serial number, the blue number from 0 to 100 denotes SIC (%), green number denotes SIC in the grid.

On the marginal ice zone, the average SIC of the aerial photo is 47.75%, the bias (relative error) is -23% (-48.2%). With the decrease of SIC, the relative error of AMSR-E SIC is increasing. We also note that the most underestimation (-43%) did not appear on the edge of the ice, but in the middle of high SIC of the area, this phenomenon is worthy of further investigation.

3.2 Validation of AMSR-E ASI SIC using MODIS SIC

In order to maintain the high resolution of MODIS image, tie-point method is employed to calculate MODIS SICs [11, 12]. This method is based on the relationship between surface broadband albedo and the SIC and is able to get the SIC of each pixel with 500-m spatial resolution. The formula of the broadband albedo (BBA) α is:

$$\alpha = R1 \times 0.3265 + R4 \times 0.2366 + R3 \times 0.4364$$

and R1, R4, R4 represents surface reflectance in band1, band4, band3 of MODIS. The albedo of pure water and pure ice, A_w and A_I, in the tie-point method, was set to 0.08 and 0.67 respectively according to the agreement with the SICs from the aerial image.

Then the retrieval SIC results in MODIS grid is projected into the AMSR-E 6.25 km polar stereographic grid. After region average, the MODIS SICs on AMSR-E grid is compared with SIC product from the University of Bremen. According to Fig. 4, AMSR-E SICs are consistent with MODIS SICs on the ice shelf and open water but underestimate SICs of all grids of sea ice (the average underestimate is 8.5% after removing the ice shelf). Previous studies have inferred that the underestimation of AMSR-E SICs in low SIC area mainly results from thin ice or new ice. Besides, the sea ice flooding caused by thick snow is also a common underestimate factor in Antarctica.

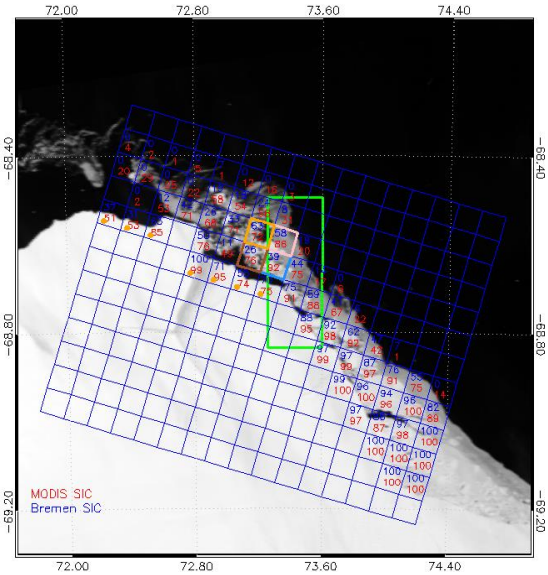

Fig. 4. SICs of AMSR-E and Aqua MODIS, blue rectangular is AMSR-E grid, blue and red number is AMSR-E and Aqua MODIS SIC.

3.3 Comparisons between SIAs and SIEs from three different SIC algorithms

DT-ASI algorithm of SIC has been achieved in the Arctic by Hao and Su [5] base on dynamic algorithms suitable to SSMI/SSMR data [13]. In this work, The SIE and SIA result from ASI (Bremen University), DT-ASI, as well as Nasa Team (NT) algorithm from NSIDC were compared. From Fig. 5., the two ASI SIE results are similar. Both ASI and SIE are less than NT results during December to June, while a little larger than NT results during the middle of September to the end of October. For the SIA result, because of the different size of pole hole in the central Arctic of different microwave sensor, we here just compared two SIA results from ASI and DT-ASI algorithms.

The SIA and SIE differences in 2016 are an order of magnitude less than the original value. SIE from DT-ASI is basically larger than that from UB ASI with larger bias

in winter than in summer. The maximum and minimum of bias occur in January (1.77×10^5 km^2) and August (1.70×10^3 km^2), respectively and the mean bias is 9.92×10^4 km^2. For SIA from DT-ASI only shows obvious less than that of ASI in February and June. The mean bias approximates to 3.14×10^4 km^2.

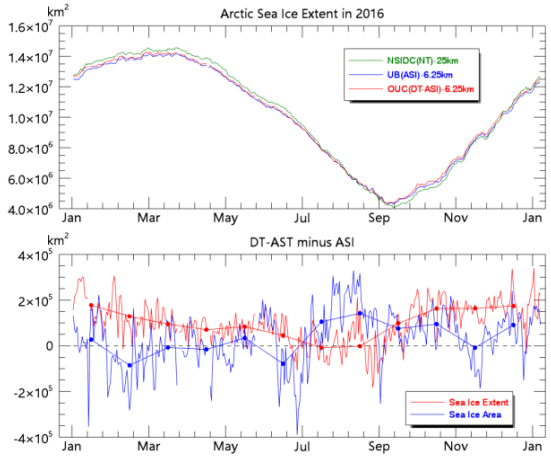

Fig.5. The plot of the SIE from three different SIC algorithms (above panel) and differences of SIAs and SIEs derived from two ASI SICs (below panel)

4. DISCUSSIONS AND CONCLUSION

With the wide application of AMSR-E high-resolution sea ice concentration products, the evaluation and verification of these products have become a very important issue. In this paper, we use SICs extracted from the high-resolution aerial image as well as MODIS image to validate AMSR-E ASI SIC products.

Compared with the SICs from the aerial image, the daily mean AMSR-E products underestimate SICs about 17.9% after excluding open water. On grids mixed by ice shelf and open water, AMSR-E SIC is generally consistent with the SICs of the aerial image; but in region consists of trash ice, AMSR-E underestimates the SICs from 13% to 43% and the average underestimation approximates to 26%. Compared with the validated SICs from MODIS image, AMSR-E product also underestimates the SICs and the overall underestimation approximates to 8.5% on average.

SIE results of both two ASI algorithm are less than that of NT results during December to June, only a little larger than that of NT results during the middle of September to the end of October. In general, the SIE and SIA derived from DT-ASI is 9.92×10^4 km^2 and 3.14×10^4 km^2 higher than that from ASI SICs. The SIE biases mainly occur in winter while SIA bias mainly occurs in summer, which means SICs of DT-ASI are higher than that of ASI particularly in summer.

ACKNOWLEDGEMENTS

This work was supported by the National Key Research and Development Program of China (2016YFC1402705) and the Global Change Research Program of China (2015CB953901) and the National Natural Science Foundation of China (No.41330960).

REFERENCES

[1] J. C. Comiso and D. K.Hall, "Climate trends in the Arctic as observed from space," *WIREs Clim Change,* vol. 5, pp. 389-409, 2014.

[2] J. C. Comiso, C. L. Parkinson, R. Gersten, et al. "Accelerated decline in the Arctic sea ice cover", Ge*ophys. Res. Lett.,* 35, L01703, 2008.

[3] V. Livina and T. Lenton, "A recent tipping point in Arctic sea-ice over: abrupt and persistent increase in the seasonal cycle since 2007". *Cryosphere*, vol.7: pp. 275–286, 2013.

[4] G. Spreen, L, Kaleschke, and G. Heygster, "Sea ice remote sensing using AMSR-E 89-GHz channels," *Journal of Geophysical Research,* vol.113, pp. 447-453, 2008.

[5] G. Hao and J. Su, "A study on the dynamic tie points ASI algorithm in the Arctic Ocean", *Acta Oceanologica Sinica*, 34(11): pp. 126-135, 2015.

[6] N. Ivanova, O. M. Johannessen, L. T. Pedersen, et al., "Retrieval of Arctic Sea Ice Parameters by Satellite Passive Microwave Sensors: A Comparison of Eleven Sea Ice Concentration Algorithms," *IEEE Transactions on Geoscience & Remote Sensing*, vol. 52, no. 11, pp. 7233-7246, April. 2014.

[7] H. Wiebe, G. Heygster, and T. Markus, "Comparison of the ASI Ice Concentration Algorithm With Landsat-7 ETM+ and SAR Imagery", *IEEE Transactions on Geoscience and Remote Sensing*, 47(9): pp. 3008-3015, 2009.

[8] X. Ying, S. Bo, and L. Xin, "Assessment of AMSR-E ASI sea ice concentration using ship observations and Landsat-7 ETM+ imagery", *Journal of Remote Sensing* (in Chinese), 17(3): pp. 514-526, 2013.

[9] X. Zhao, H. Su, A. Stein, and X. Pang, "Comparison between AMSR-E ASI sea-ice concentration product, MODIS and pseudo-ship observations of the Antarctic sea-ice edge", *Annals of Glaciology*, 56(69): pp. 45-52, 2015.

[10] J. Kittler and J. Illingworth, "Minimum error thresholding". *Pattern recognition*, 19(1): pp. 41-47, 1986.

[11] J. Su, G. Hao, X.Ye, and W. Wang, "The experiment and validation of sea ice concentration AMSR-E retrieval algorithm in the polar region", *Journal of Remote Sensing*, 17(3): pp. 495-513, 2013.

[12] G. Hao and J. Su, "A study on the dynamic tie points ASI algorithm in the Arctic Ocean", *Acta Oceanologica,* 34(11): pp. 126-135, 2015.

[13] S. Eastwood, K. R. Larsen, T. Lavergne, E. Nielsen, 13Reprocessing Product User Manual", Ver.1.3, *EUMETSAT*, 2011.